

PREPARATION AND CHARACTERIZATION, OF LIGAND COMPLEXES OF DI-BETA-ENAMINO WITH SOME METALS

Qader Abdullah Shanak, Nabil Jamal Alasli, Ahmed Thabit Numan

Chemistry Department - College of Education for Women - Tikrit University. Salah Al-Din – Iraq.

Abstract: This study includes preparing one ligand and then complicating them with some metals. The ligand (L_3) was prepared by mixing the ligand (L_1) with 3-aminophenol, grinding them, and then performing the melting process. Preparation of complexes of cobalt Co(II), nickel Ni(II), copper Cu(II), zinc Zn(II), cadmium Cd(II) with ligand (L_3) and 3-aminophenol through reacting metal salts with ligand (L_3) and 3-aminophenol and using ethanol as a solvent. The validity of the structures was confirmed by physical and spectroscopic methods of the prepared ligands and complexes, such as electrical conductivity, magnetic sensitivity, melting points, UV-Vis spectrum, infrared (FT-IR), nuclear magnetic resonance spectra of the proton and carbon ($^1\text{H-NMR}$), ($^{13}\text{C-NMR}$).

Keywords: *Ligand, Complex, 3-Aminophenol.*

1. Introduction:

β -enaminone is one of the most important compounds that play an important role in organic synthesis, which is considered a raw material in the preparation of biologically effective compounds [1], which are used as anticonvulsants and inhibitors such as (oxytocin) and inhibitors [2], acetylcholine-esters [3]. Where researchers were able to prepare it usually from the reaction of aliphatic and aromatic amines with (β -dicarbonyl) compounds and in the presence of some high-efficiency cofactors [4]. The efficiency of the catalysts used in the preparation of β -enaminone was examined by condensation reactions between aniline and timid one and by thermal smelting [5]. In the year (1864) German chemist Hugo Schiff developed a new class of organic compounds resulting from a condensation reaction between aldehydes or ketones with primary amines [6]. These compounds are called imines, and the imines became known as Schiff bases in his honor [7]. Schiff's bases have many names, including azomethines, benzanils, benzylidene aniline [8], and ketimines. (Ketimines) when derived from ketones and aldimines (Aldimines) when derived from aldehydes [9]. Schiff's bases are one of the most prominent ligands used in coordination chemistry, as they enter into the preparation of a large number of complexes with metal ions in general and with transitional elements in particular because of their ability to coordinate and form complexes with different structures and multiple uses [10]. Several studies showed the effect of the electronic double in orbital sp^2 hybrid of nitrogen atom on the basic properties of the compounds containing the imine group and the presence of the double bond of the imine group [11]. The basic ability of the group ($\text{C}=\text{N}$) is insufficient to form stable complexes. Hence, the presence of effective

groups such as OH, SH, or NH near the imine group is necessary to form stable complexes with metal ions [12]. Therefore, Schiff bases are considered among the important chelating ligands in forming many coordination complexes that show diverse patterns of bonding, some of which are in the form of bidentate ligands. Some of them are Bidentate ligands. In the form of tridentate ligands or polydentate ligands: Tetradentate ligands, Pentadentate ligands [13], Hexadentate ligands [14]. The properties and stability of Schiff bases are often closely related to carbonyl compounds and amines derived from them, whether aliphatic or aromatic [15].

2. Experimental:

2.1. Chemicals used: All chemicals used in this work were purchased from BDH, Aldrich and Fluka companies and were used without further purification.

2.2. Devices used: The melting points were measured using Electrothermal Melting Apparatus 9300. The FT-IR spectra were captured using a Shimadzu FT-IR 8400S spectrophotometer with a (400-4000) cm^{-1} by KBr disc. DMSO- d_6 as solvents were used to capture $^1\text{H-NMR}$ and $^{13}\text{C-NMR}$ spectra on Bruker instruments running at 400 MHz.

2.3. Ligand preparation (L3) [16, 17]:

(0.4g, 1 mmole) The Ligand (L1) was then added to it (0.1g, one mmole) of 3-aminophenol, and the mixture was crushed in a ceramic jar until it became a powder. Then the melting process was conducted in the convection oven at 170°C for half an hour to complete the reaction. The mixture was taken out of the oven after its melting was complete and its color became dark brown, and then it was washed with gasoline and left to dry for 24 hours. It gave a dark brown precipitate with a weight of (0.38 gm) and a percentage of (92%) with a melting point of (317-315) $^\circ\text{C}$.

2.4. Preparation of the Co (II) cobalt complex with ligand [L3] and 3-aminophenol [18]:

In a round-bottom flask (100 ml), put (0.77 gm, two moles) of metallic salt chloride ($\text{CoCl}_2 \cdot 6\text{H}_2\text{O}$) dissolved in (10 ml) of ethanol with Stirring for ten minutes, then (0.11 gm, one mmole) of (L3) dissolved in 10 ml) of ethanol was added to it, and (0.035 gm) of ethanol was dissolved, two moles of 3-aminophenol with ethanol, then (3-4) drops of potassium hydroxide was added to become the $\text{pH}=8-9$. The mixture was left for the reflux escalation process for (4 hr), the solution was filtered while hot, a light green precipitate was obtained, then washed with gasoline, then dried and weighed ($\text{Wt}=0.083$ gm), and the resulting complex was (83%).

The complexes were prepared as indicated in paragraphs (2.4.) and with the same quantities of ligand [L3]. Table (1) shows the amount of metal salt used in preparing the complex and the molecular formulas of the complexes. The prepared preparation, its weights, and the color of the resulting complex.

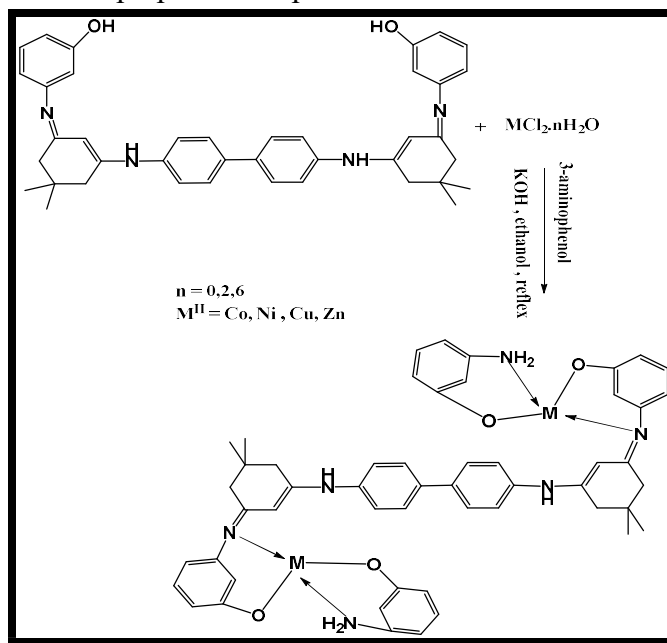
Table (1): mixed [L3] complexes and quantities of metal salts used in their preparation

Metal salt	Wt. of salt (g) 2mmol	Wt. of L ₁ (g) 1mmol	Weight of 3-aminophenol (g) 2mmol	Complexes L ₃	Color	Yield %
$\text{CoCl}_2 \cdot 6\text{H}_2\text{O}$	0.077	0.11	0.035	$[(\text{Co})_2 (\text{L}_3) (3\text{ph})_2]$	Dark brown	83
$\text{NiCl}_2 \cdot 6\text{H}_2\text{O}$	0.077	0.11	0.035	$[(\text{Ni})_2 (\text{L}_3) (3\text{ph})_2]$	Dark brown	91
$\text{CuCl}_2 \cdot 6\text{H}_2\text{O}$	0.055	0.11	0.035	$[(\text{Cu})_2 (\text{L}_3) (3\text{ph})_2]$	Dark brown	79
ZnCl_2	0.044	0.11	0.035	$[(\text{Zn})_2 (\text{L}_3) (3\text{ph})_2]$	Grey	77

CdCl ₂ .2H ₂ O	0.056	0.11	0.035	[(Cd) ₂ (L ₃) (3ph) ₂]	Light green	87
--------------------------------------	-------	------	-------	---	-------------	----

3. Results and discussion:

The complexes of L3 ligands mixture with metal ions (Co, Ni, Cu, Zn, Cd) were prepared. Spectroscopic and analytical methods characterized the prepared complexes.



Scheme (1): Preparation of mixed ligand (L3) complexes.

3.1. Nuclear magnetic resonance (¹H-NMR) spectrum of the Ligand (L3):

The (¹H-NMR) spectrum of the ligand (L3) was recorded according to figure (1), as it showed a single signal at (8.89) ppm belonging to the (OH) group protons. The single signal at ppm (8.81) belongs to the (NH) group protons, the multiple signals at ppm (6.58-7.69) are due to the aromatic ring protons, and the single signal appears at ppm (5.21-5.42) refers to the proton of the group (CH) next to the group (C=C), and the appearance of a single signal at ppm (3.36) refers to the protons of the water molecule, as well as the appearance of signals at ppm (2.51 and 2.52) refers to the protons of the solvent (DMSO-d₆), and the appearance of a single signal at ppm (2.09 and 2.10) refers to the protons of the two groups (CH₂) adjacent to the group (C=C), and the appearance of a single signal at ppm (1.92 and 2.07) refers to the protons of the two (CH₂) groups adjacent to the azomethine group, and finally the signal at ppm (1.00, 1.02, 1.04 and 1.05) belongs to Groups of protons (CH₃) [19, 20].

3.2. Nuclear magnetic resonance (¹³C-NMR) spectrum of the ligand (L3):

As for the spectrum of the ligand (L3), according to figure (2), it was observed that a signal at ppm (162.32) belonged to C-OH carbon), and a signal appeared at ppm (158.53) that returned to the carbon of the azomethine group, and the appearance of two signs at ppm (152.44 and 150.32) belonging to the carbon of the (C=C) group, and the appearance of multiple signs at ppm (97.90 - 147.32) belonging to the carbons of the aromatic rings, and the appearance of two signals at ppm (60.12 and 54.19) belonging to the carbon of the two groups

(CH₂) adjacent to the olefinic group (C=C), and the appearance of two signals at ppm (49.96 and 43.78) due to the carbon of two groups (CH₂) next to the azomethine group, as well as the appearance of a signal at ppm (39.48 - 43.48) due to the solvent (DMSO-d₆), and the appearance of a single signal ppm (32.43) due to the carbons of two groups (C-CH₃), and the appearance of single ppm signals (30.19, 27.40, 21.29 and 14.95) belong to the carbons of groups (CH₃) [21, 22].

3.3. Molar Electrical Conductivity

The purpose of measuring electrical conductivity is to derive the ionic formula of a complex in a solution or solid-state. In this research, the molar electrical conductivity of the prepared complexes was measured at a concentration of (10⁻³ molar) in dimethyl sulfur dioxide solvent and laboratory temperature [23, 24]. Table (2) shows the prepared complexes' electrical conductivity values and molarity.

Table (2): The values of molar electrical conductivity (cm²/ohm.mol) for the complexes prepared at a temperature of 25°C and a concentration of (10⁻³ molarity) in a DMSO solvent.

Complex	Λ _m (S.cm ² . mol ⁻¹)
	In DMSO
[(Co) ₂ (L ₃) (3ph) ₂]	.7815
[(Ni) ₂ (L ₃) (3ph) ₂]	.5517
[(Cu) ₂ (L ₃) (3ph) ₂]	.4318
[(Zn) ₂ (L ₃) (3ph) ₂]	.7714
[(Cd) ₂ (L ₃) (3ph) ₂]	.8311

3.4. Magnetic Measurements

The expected value of the magnetic moment for cobalt (II) tetrahedral complexes ranges from (4.10-4.80 B.M), which is greater than (B.M.3.82) due to the presence of an orbital contribution. The prepared homogeneous bi-nuclear cobalt (II) complexes showed magnetic moments within the range (4.38 -4.73 B.M), and these values are generally in agreement with the tetragonal cobalt (II) complexes Surfaces (187-185) [25, 26].

The octahedral and tetrahedral nickel (II) complexes are derived from the ionic state (d⁸) and have two single electrons. Within (B.M 2.83) (123) In the case of tetrahedral complexes, the presence of the orbital contribution is a source of increasing the value of the magnetic moment to (B.M 4.0) (124). (II) prepared homogeneous dinuclear magnetic moments within the range (3.96-3.98 B.M), and these values are in general agreement with the tetrahedral nickel (II) complexes [27, 28].

The prepared homogeneous binuclear copper (II) complexes gave magnetic moments in the range (2.00-2.10 B.M), and these values are generally in agreement with the tetragonal copper (II) complexes Surfaces [29, 30]. As for the zinc (II) and cadmium (II) complexes, they are magnetic dia because they have a full d orbital, and based on Raman studies and X-ray diffraction of the previously studied compounds containing negative ion (I, Br, Cl=X)[ZnX₄] was found to have a tetrahedral structure [31, 32].

Table (3): values of the effective magnetic moment μ_{eff} for the prepared complexes

Complexes	$X_g \times 10^{-6}$	$X_M \times 10^{-6}$	$X_A \times 10^{-6}$	$\mu_{\text{eff.}}$ B.M.	$D \times 10^{-6}$	S. structure
$[(\text{Co})_2 (\text{L}_3) (\text{3ph})_2]$	1.892	1782.6 6	2100.2 4	4.73	317.58	Td
$[(\text{Ni})_2 (\text{L}_3) (\text{3ph})_2]$	0.759	714.23	1031.8 1	3.96	317.58	Td
$[(\text{Cu})_2 (\text{L}_3) (\text{3ph})_2]$	0.371	353.72	671.30	2.00	317.58	Td

3.5. U.V-Vis Spectra for (L3) and their prepared complexes

The electronic spectrum of the ligand (L3) shown in figure (3) recorded two absorption peaks of the first at (230) nm (43478) cm^{-1} , ($\epsilon_{\text{max}} = 2283 \text{ (M}^{-1} \cdot \text{cm}^{-1})$ and the second at (269) nm), (37174) cm^{-1} , ($\epsilon_{\text{max}}=2196 \text{ M}^{-1} \cdot \text{cm}^{-1}$) was attributed These beams are referred to as ($\pi \rightarrow \pi^*$) and ($n \rightarrow \pi^*$) electron transitions, respectively [33].

1- Cobalt complex $[(\text{Co})_2 (\text{L}_3)(\text{3ph})_2]$

The electronic spectrum, as in figure (4), for the cobalt complex, showed four absorption peaks, the first and second peaks appearing at wavelength 301 nm (33222 cm^{-1} ($\text{max}=1062 \text{ mol}^{-1} \cdot \text{cm}^{-1} \epsilon$) and (349) nm 28,653 cm^{-1} ($\text{max}=231 \text{ mol}^{-1} \cdot \text{cm}^{-1} \epsilon$) which belong to the transitions The ligand ($\pi \rightarrow \pi^*$) and the charge transfer spectrum (C.T.), respectively, and the third and fourth peaks show two broad bands at length (600) nm (16666 cm^{-1}). ($\text{max} = 112 \text{ Mol}^{-1} \cdot \text{cm}^{-1} \epsilon$ and 983) nm) (10,172 cm^{-1} ($\text{max}= 4 \text{ Mol}^{-1} \cdot \text{cm}^{-1}$) ϵ (which refers to electronic transmission $4A_2(F) \rightarrow 4T_1(p)$ and $4A_2(F) \rightarrow 4T_1(F)$, respectively.

2- Nickel complex $[(\text{Ni})_2(\text{L}_3)(\text{3ph})_2]$

The U.V. and visible spectrum of the nickel complex (5) showed three absorption peaks of the first and second peaks at (291) nm (34,364) cm^{-1} ($\text{max}=1547 \text{ mol}^{-1} \cdot \text{cm}^{-1} \cdot \epsilon$) and (345) nm (28,985 cm^{-1} ($\text{max}=2122 \text{ mol}^{-1} \cdot \text{cm}^{-1} \cdot \epsilon$), which belong to the transitions the ligand ($\pi \rightarrow \pi^*$) and the charge transfer spectrum (C.T.), respectively, and the third peak at the wavelength (984) nm (10162 cm^{-1} ($\text{max}=3 \text{ Mol}^{-1} \cdot \text{cm}^{-1} \epsilon$) (which goes back to the electron transition $3T_1(F) \rightarrow 3T_2(F)$.

3- Copper complex $[(\text{Cu})_2(\text{L}_3)(\text{3ph})_2]$ (156):

As for the copper complex, the UV-visible spectrum showed three absorption peaks in the form (6), the first peak at ($\epsilon_{\text{max}}=2366 \text{ M}^{-1} \cdot \text{cm}^{-1}$, (37133) cm^{-1} , (265) nm, and the second peak is 21367) cm^{-1} , (468) nm) ($\epsilon_{\text{max}}=149 \text{ M}^{-1} \cdot \text{cm}^{-1}$) The origin of these peaks is attributed to the ligand transitions ($\pi \rightarrow \pi^*$) and the charge transfer spectrum (C.T.), respectively, and the third peak appeared at (778) nm, (12853) cm^{-1} , ($\epsilon_{\text{max}}=74 \text{ M}^{-1} \cdot \text{cm}^{-1}$) The origin of this peak can be traced back to the $2T_2 \rightarrow 2E$ electron transition.

4- Zinc complex $[(\text{Zn})_2(\text{L}_3)(\text{3ph})_2]$

Electronic spectrum figure (7) for the zinc complex showed two absorption peaks, and the first one appears at the wavelength 289) nm (34602 cm^{-1} ($\text{max}=207 \text{ Mol}^{-1} \cdot \text{cm}^{-1}$) ϵ (-1), which belongs to the ligand transitions ($\pi \rightarrow \pi^*$) and the second peak appears at the wavelength, (356) nm (28089 cm^{-1}). $\text{max}=134 \text{ Mol}^{-1} \cdot \text{cm}^{-1} \cdot \epsilon$) returns and the charge-transfer spectrum (C.T.).

Table (4): values of the electronic spectra of (L3) and its prepared complexes in unit (cm-1).

Compound	λ_{\max} (nm)	Wave number (cm^{-1})	ϵ_{\max} ($\text{L. mol}^{-1} \cdot \text{cm}^{-1}$)	Transition Assignment
L₃	230	43478	2283	$\pi - \pi^*$
	299	37174	2196	$n - \pi^*$
[(Co)₂ (L₃) (3ph)₂]	301	33222	1062	$\pi - \pi^*$
	349	28653	231	C.T
	600	16666	112	${}^4A_{2(F)} \rightarrow {}^4T_{1(P)}$
	983	10172	4	${}^4A_{2(F)} \rightarrow {}^4T_{1(F)}$
[(Ni)₂ (L₃) (3ph)₂]	291	34364	1547	$\pi - \pi^*$
	345	28985	2122	C.T
	984	(10162)	3	${}^3T_{1(F)} \rightarrow {}^3T_{2(F)}$
[(Cu)₂ (L₃) (3ph)₂]	265	37735	2366	$\pi - \pi^*$
	468	21367	149	C.T
	778	12853	74	${}^2T_2 \rightarrow {}^2E$
[(Zn)₂ (L₃) (3ph)₂]	289	34602	207	$\pi - \pi^*$
	356	28089	134	C.T C.T

3.6. FT-IR spectrum for the ligand (L3) and their prepared complexes

The infrared spectra of the prepared complexes shown in figures (8)-(11) showed absorption bands between about cm^{-1} (1612-1597) due to the $\nu(\text{C}=\text{N})$ band shifted to a lower frequency than it was in the free state of [L3] figure (8), which was of the order of $\nu(\text{C}=\text{N})=1654 \text{ cm}^{-1}$. The displacement in the beam is evidence of the coordination of the metal ions and their association with the nitrogen atom of the $\nu(\text{C}=\text{N})$ group in the [L3] ligand. This connection is reinforced by the fact that the appearance of weak absorption bands between (cm^{-1} 1486) and (1555 cm^{-1}) is due to the $\nu(\text{M}-\text{O})$ bond in the complexes [34, 35].

The infrared spectrum of the complexes also showed the disappearance of the absorption bands of the $\nu(\text{OH})$ group in the complexes compared to the ligand, and this indicates the coordination of the metal ions with the oxygen atom of the $\nu(\text{OH})$ group in the [L3] ligand. In addition to the appearance of two absorption bands between cm^{-1} (3360-3182) for all the above complexes attributed to the group $\nu(\text{NH}, \text{NH}_2)$, it also showed some absorption bands. Between cm^{-1} (1535-1554) is attributed to the $\nu(\text{C}=\text{C})$ function [36]. The results are shown in table (5).

Table (5): The locations of the main absorption beams of the infrared spectra of the mixed ligand (L3) complexes with unit Cm^{-1} .

Compound	$\nu(\text{NH}_2)$ & $\nu(\text{OH})$	$\nu(\text{C}=\text{N})$	$\nu(\text{C}=\text{C})$	$\nu(\text{N}-\text{H})$	$\nu(\text{M}-\text{N})$	$\nu(\text{M}-\text{O})$
[L ₃]	3369 br	1654 s	1555 sh	3244 sh	----	----
[(Co) ₂ (L ₃) (3ph) ₂]	3267 sh 3221 sh	1612 s	1554 sh 1535 sh	3286 sho	528 w	455w
[(Ni) ₂ (L ₃) (3ph) ₂]	3248 sh 3182 s	1604 sh	1552 sho 1535 s	3140 s	555 w	455 w
[(Cu) ₂ (L ₃) (3ph) ₂]	3267 sh 3196 s	1633 sh	1562 sh 1538 s	3154 s	507 w	460 w
[(Zn) ₂ (L ₃) (3ph) ₂]	3360 sh 3294 sh	1597 sh	1550 sho 1539 sho	3186 s	486 w	455w

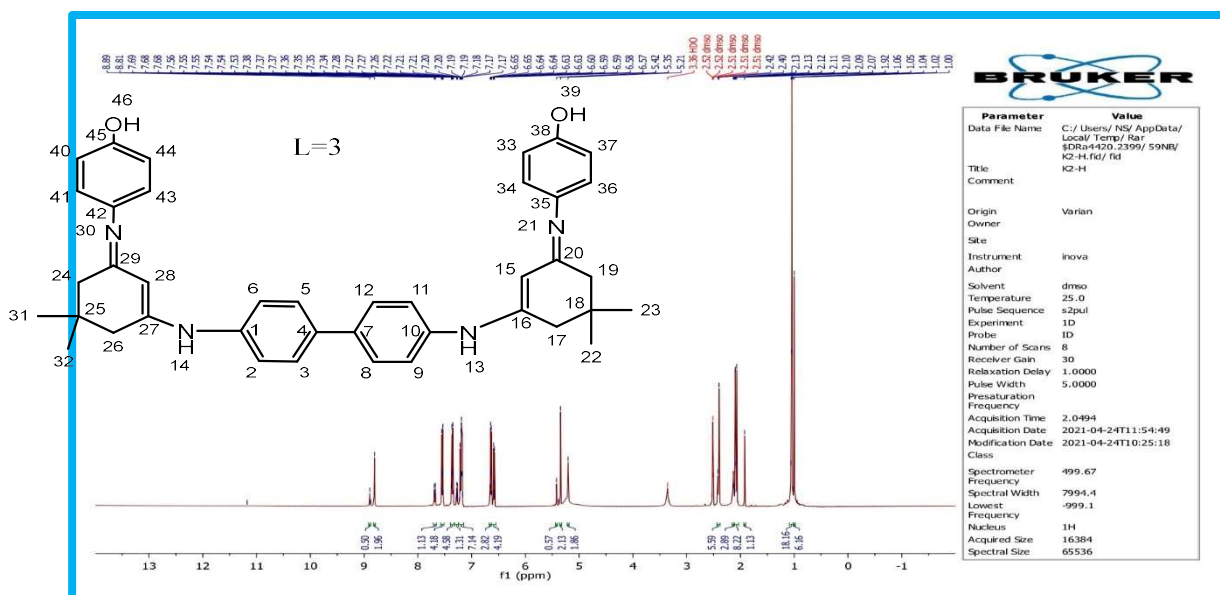


Figure (1): $^1\text{H-NMR}$ spectrum of the (L₃)

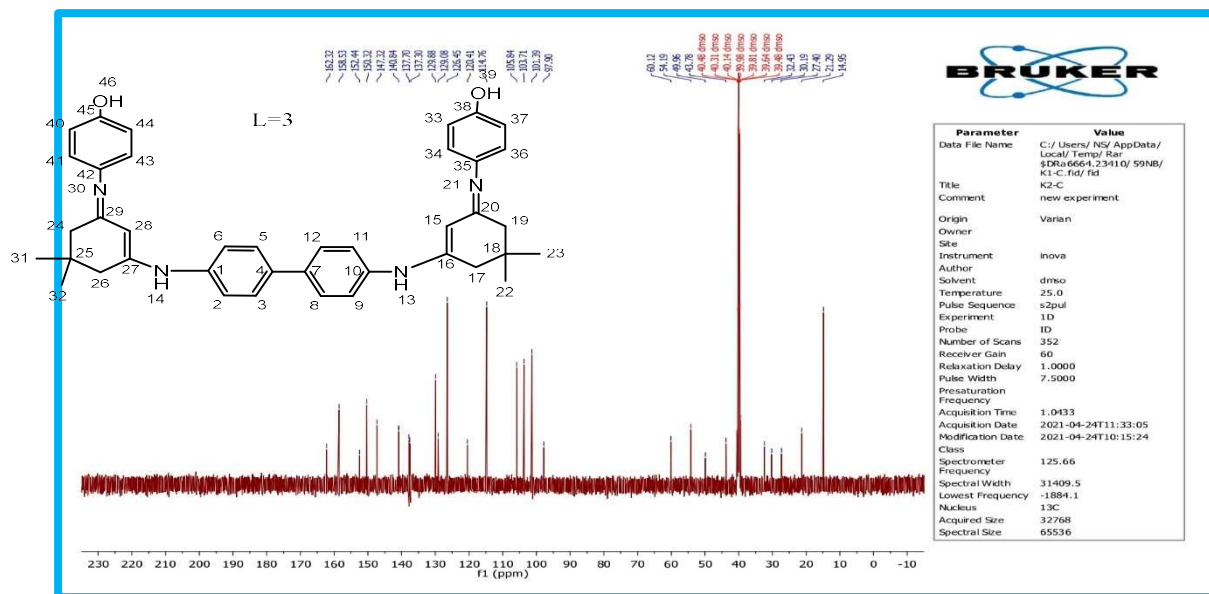


Figure (2): ¹³C-NMR spectrum of the (L3)

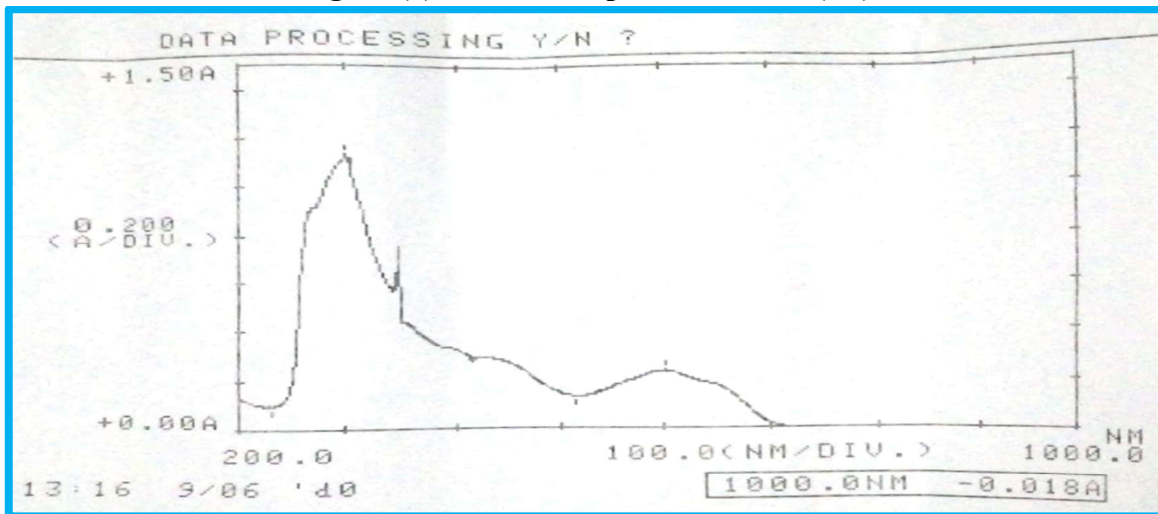


Figure (3): UV spectrum of the (L3)

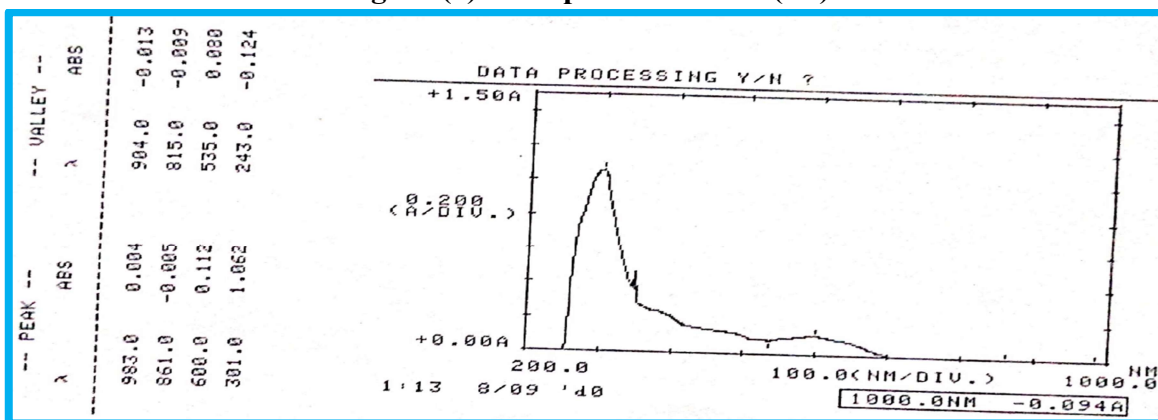


Figure (4): UV spectrum of complex [(Co)₂(L3)(3ph)₂]

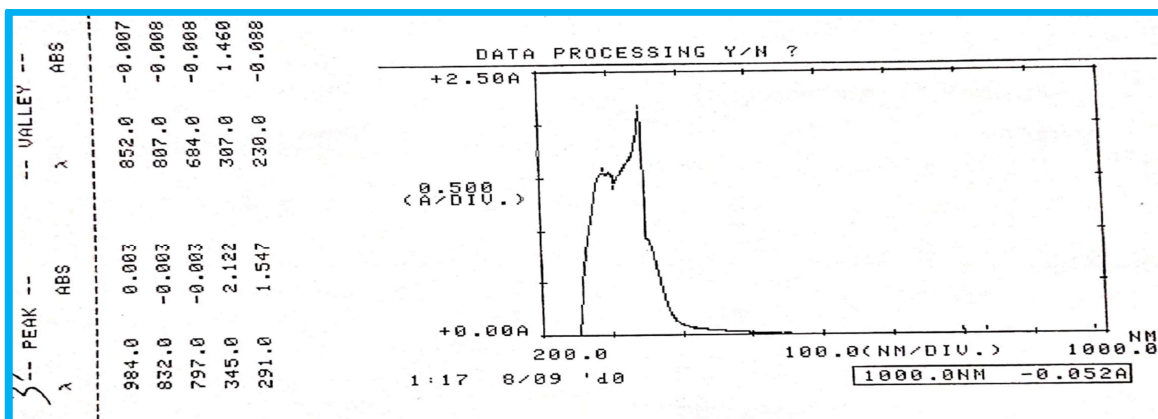


Figure (5): UV spectrum of complex $[(Ni)_2 (L_3) (3ph)_2]$

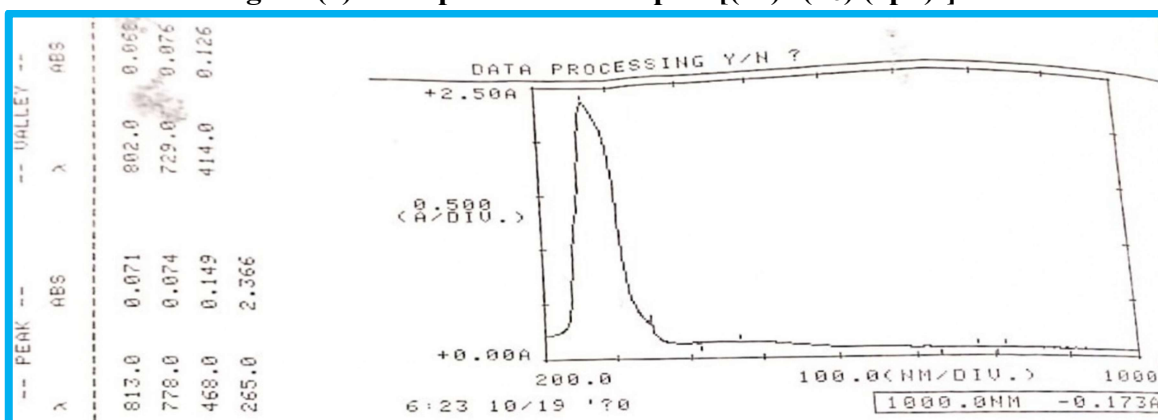


Figure (6): UV spectrum of complex $[(Cu)_2 (L_3) (3ph)_2]$

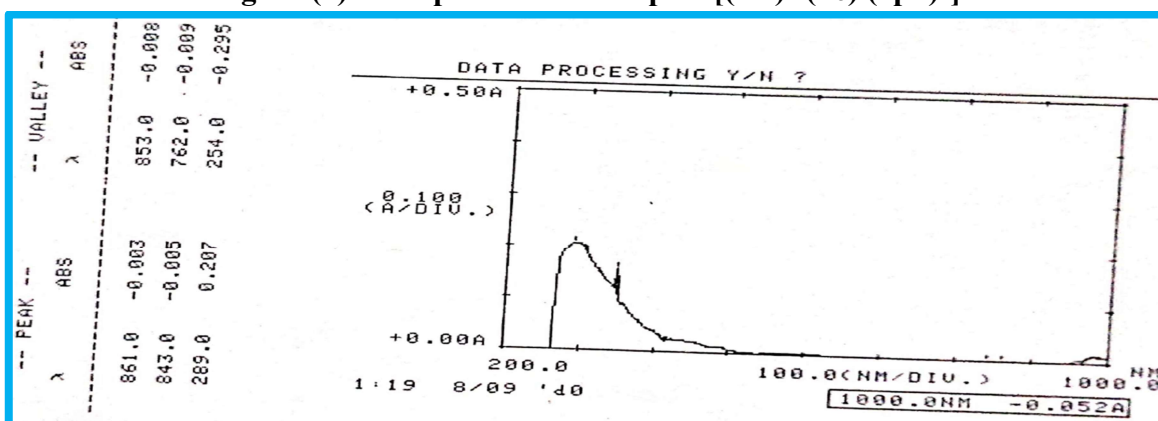


Figure (7): UV spectrum of complex $[(Zn)_2 (L_3) (3ph)_2]$

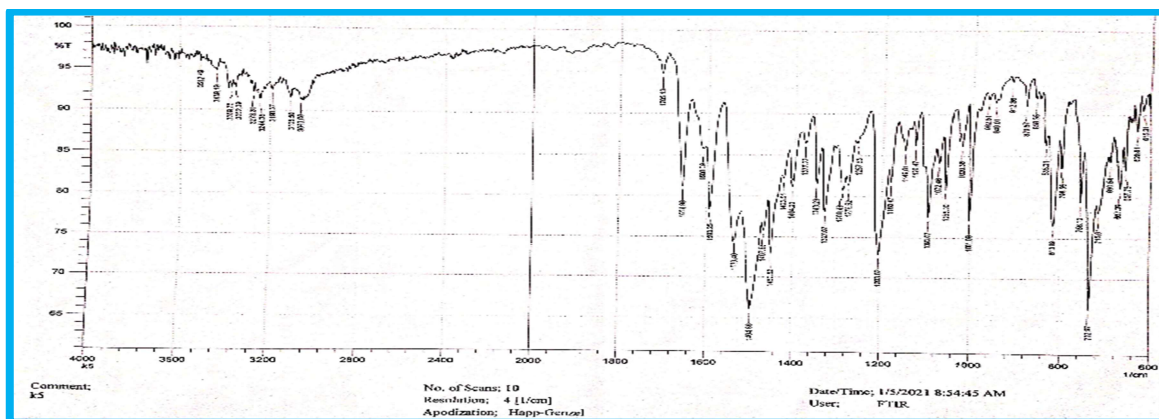


Figure (8): Infrared spectrum of (L3)

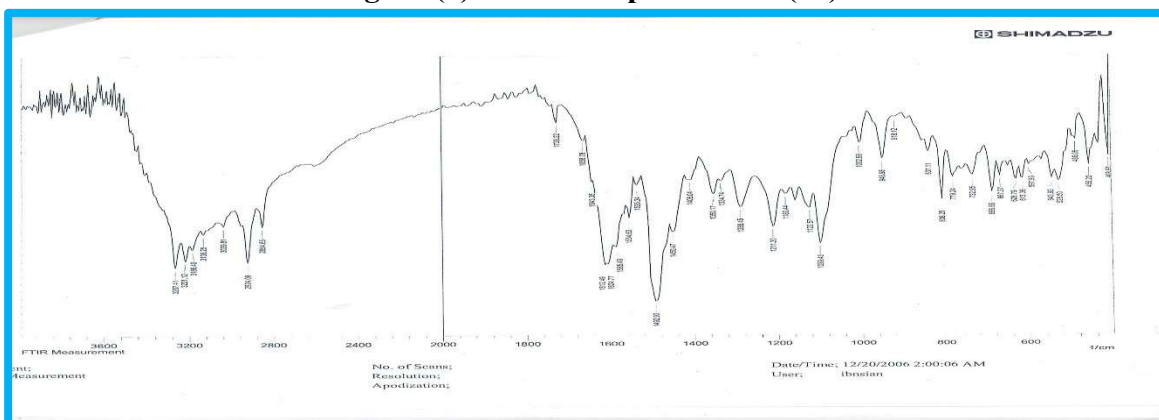


Figure (9): Infrared spectrum of [(Co)₂ (L₃) (3ph)₂]

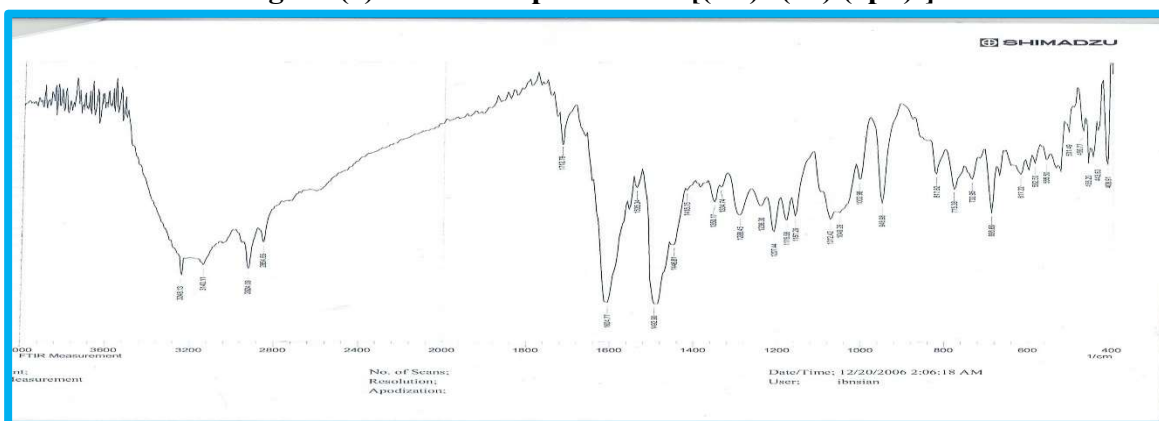


Figure (10): Infrared spectrum of [(Ni)₂ (L₃) (3ph)₂]

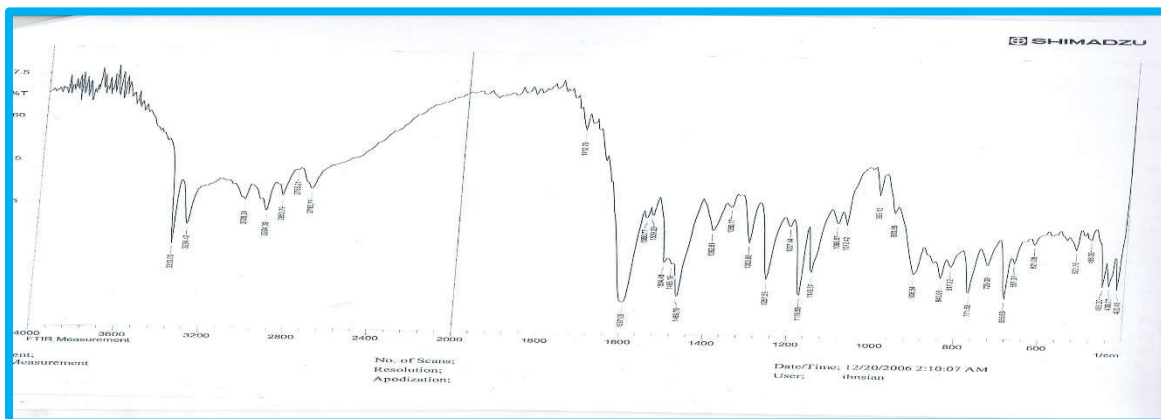


Figure (11): Infrared spectrum of [(Zn)₂ (L₃) (3ph)₂]

4. Conclusions: The laboratory and spectroscopic measurements proved the validity and accuracy of the prepared ligands and complexes. II) is tetrahedral. The measurements also proved that the nickel (II) complexes are tetrahedral. The measurements proved that the copper (II) complexes are tetrahedral. The measurements proved that the zinc (II) complexes were tetrahedral. The measurements proved that the cadmium (II) complexes are tetrahedral. All the prepared complexes were colored. In addition, it appeared through the biological study that most of the prepared complexes had anti-bacterial activity and could inhibit the growth of bacteria, as it was found that these compounds inhibit bacterial growth. higher than the control sample used in the study

Reference

1. Siddiqui, Z. N., Khan, K., & Ahmed, N. (2014). Nano fibrous silica sulphuric acid as an efficient catalyst for the synthesis of β -enaminone. *Catalysis letters*, 144(4), 623-632.
2. Suryavanshi, P. A., Sridharan, V., & Menéndez, J. C. (2013). A β -enaminone-initiated multicomponent domino reaction for the synthesis of indoloquinolizines and benzoquinolizines from acyclic precursors. *Chemistry–A European Journal*, 19(39), 13207-13215.
3. Bhattacharjee, D., Ram, S., Chauhan, A. S., & Das, P. (2019). Hypervalent Iodine (III)-Mediated Counteranion Controlled Intramolecular Annulation of Exocyclic β -Enaminone to Carbazolone and Imidazo [1, 2-a] pyridine Synthesis. *Chemistry–A European Journal*, 25(23), 5934-5939.
4. De Vreese, R., Grootaert, C., D'hoore, S., Theppawong, A., Van Damme, S., Van Bogaert, M., & D'hooghe, M. (2016). Synthesis of novel curcuminoids accommodating a central β -enaminone motif and their impact on cell growth and oxidative stress. *European journal of medicinal chemistry*, 123, 727-736.
5. Shi, L., Xue, L., Lang, R., Xia, C., & Li, F. (2014). Four-Component Synthesis of β -Enaminone and Pyrazole through Phosphine-Free Palladium-Catalyzed Cascade Carbonylation. *ChemCatChem*, 6(9), 2560-2566.
6. Sinn, E., & Harris, C. M. (1969). Schiff base metal complexes as ligands1. *Coordination Chemistry Reviews*, 4(4), 391-422.
7. Gupta, K. C., & Sutar, A. K. (2008). Catalytic activities of Schiff base transition metal complexes. *Coordination Chemistry Reviews*, 252(12-14), 1420-1450.

8. Yamada, S. (1999). Advancement in stereochemical aspects of Schiff base metal complexes. *Coordination Chemistry Reviews*, 190, 537-555.
9. Cordes, E. H., & Jencks, W. P. (1962). On the mechanism of Schiff base formation and hydrolysis. *Journal of the American Chemical Society*, 84(5), 832-837.
10. Xavier, A., & Srividhya, N. (2014). Synthesis and study of Schiff base ligands. *IOSR Journal of Applied Chemistry*, 7(11), 06-15.
11. Cozzi, P. G. (2004). Metal–Salen Schiff base complexes in catalysis: practical aspects. *Chemical Society Reviews*, 33(7), 410-421.
12. Jia, Y., & Li, J. (2015). Molecular assembly of Schiff base interactions: construction and application. *Chemical reviews*, 115(3), 1597-1621.
13. Zhang, J., Xu, L., & Wong, W. Y. (2018). Energy materials based on metal Schiff base complexes. *Coordination Chemistry Reviews*, 355, 180-198.
14. Pervaiz, M., Sadiq, S., Sadiq, A., Younas, U., Ashraf, A., Saeed, Z., & Adnan, A. (2021). Azo-Schiff base derivatives of transition metal complexes as antimicrobial agents. *Coordination Chemistry Reviews*, 447, 214128.
15. Sun, Y., Lu, Y., Bian, M., Yang, Z., Ma, X., & Liu, W. (2021). Pt (II) and Au (III) complexes containing Schiff-base ligands: A promising source for antitumor treatment. *European Journal of Medicinal Chemistry*, 211, 113098.
16. El-Gammal, O. A., Mohamed, F. S., Rezk, G. N., & El-Bindary, A. A. (2021). Structural characterization and biological activity of a new metal complexes based of Schiff base. *Journal of Molecular Liquids*, 330, 115522. El-Gammal, O. A., Mohamed, F. S., Rezk, G. N., & El-Bindary, A. A. (2021). Synthesis, characterization, catalytic, DNA binding and antibacterial activities of Co (II), Ni (II) and Cu (II) complexes with new Schiff base ligand. *Journal of Molecular Liquids*, 326, 115223.
17. Dalaf, A. H. (2018). Synthesis and Characterization of Some Quartet and Quinary Hetero cyclic Rings Compounds by Traditional Method and Microwave Routes Method and Evaluation of Their Biological Activity. *M.Sc. Thesis, Tikrit University, Tikrit, Iraq*: 1-94 pp.
18. Dalaf, A. H., & Jumaa, F. H. (2018). Synthesis, Characterization of some 1,3-Oxazepane -4,7-Dione by Traditional and Microwave routes method and evaluation of their biological activity. *Al-utroha for Pure Science*. (8): 93-108.
19. Dalaf, A. H., Jumaa, F. H., & Jabbar, S. A. S. (2018). Synthesis and Characterization of some 2, 3-dihydroquinoxoline and evaluation of their biological activity. *Tikrit Journal of Pure Science*, 23(8): 66-67. <http://dx.doi.org/10.25130/tjps.23.2018.131>.
20. Salwa, A. J., Ali, L. H., Adil, H. D., Hossam, S. A. (2020). Synthesis and Characterization of Azetidine and Oxazepine Compounds Using Ethyl-4-((4-Bromo Benzylidene) Amino) Benzoate as Precursor and Evaluation of Their Biological Activity. *Journal of Education and Scientific Studies*, ISSN: 24134732. 16(5): 39-52.
21. Abd, I. Q., Ibrahim, H. I., Jirjes, H. M., & Dalaf, A. H. (2020). Synthesis and Identification of new compounds have Antioxidant activity Beta-carotene, from Natural Auxin Phenyl Acetic Acid. *Research Journal of Pharmacy and Technology*, 13(1): 40-46. <https://doi.org/10.5958/0974-360X.2020.00007.4>.

22. Dalaf, A. H., & Jumaa, F. H. (2020). Synthesis, Identification and Assess the Biological and Laser Efficacy of New Compounds of Azetidine Derived from Benzidine. *Muthanna Journal of Pure Science (MJPS)*, **7(2)**:12-25. DOI: [10.18081/2226-3284/14-10/12-25](https://doi.org/10.18081/2226-3284/14-10/12-25).
23. Saleh, R. H., Rashid, W. M., Dalaf, A. H., Al-Badrany, K. A., & Mohammed, O. A. (2020). Synthesis of Some New Thiazolidinone Compounds Derived from Schiff Bases Compounds and Evaluation of Their Laser and Biological Efficacy. *Ann Trop & Public Health*, **23(7)**: 1012-1031. <http://doi.org/10.36295/ASRO.2020.23728>.
24. Yass, I. A., Aftan, M. M., Dalaf, A. H., & Jumaa, F. H. (Nov. 2020). Synthesis and Identification of New Derivatives of Bis-1,3-Oxazepene and 1,3-Diazepine and Assess the Biological and Laser Efficacy for Them. *The Second International & The Fourth Scientific Conference of College of Science – Tikrit University*. (P4): 77-87.
25. Salih, B. D., Dalaf, A. H., Alheety, M. A., Rashed, W. M., & Abdullah, I. Q. (2021). Biological activity and laser efficacy of new Co (II), Ni (II), Cu (II), Mn (II) and Zn (II) complexes with phthalic anhydride. *Materials Today: Proceedings*, **43**, 869-874. <https://doi.org/10.1016/j.matpr.2020.07.083>.
26. Aftan, M. M., Jabbar, M. Q., Dalaf, A. H., & Salih, H. K. (2021). Application of biological activity of oxazepine and 2-azetidinone compounds and study of their liquid crystalline behavior. *Materials Today: Proceedings*, **43**, 2040-2050. <https://doi.org/10.1016/j.matpr.2020.11.838>.
27. Aftan, M. M., Talloh, A. A., Dalaf, A. H., & Salih, H. K. (2021). Impact para position on rho value and rate constant and study of liquid crystalline behavior of azo compounds. *Materials Today: Proceedings*. <https://doi.org/10.1016/j.matpr.2021.02.298>.
28. Aftan, M. M., Toma, M. A., Dalaf, A. H., Abdullah, E. Q., & Salih, H. K. (2021). Synthesis and Characterization of New Azo Dyes Based on Thiazole and Assess the Biological and Laser Efficacy for Them and Study their Dyeing Application. *Egyptian Journal of Chemistry*, **64(6)**, 2903-2911. <https://dx.doi.org/10.21608/ejchem.2021.55296.3163>.
29. Khalaf, S. D., Ahmed, N. A. A. S., & Dalaf, A. H. (2021). Synthesis, characterization and biological evaluation (antifungal and antibacterial) of new derivatives of indole, benzotriazole and thioacetyl chloride. *Materials Today: Proceedings*. **47(17)**, 6201-6210. <https://doi.org/10.1016/j.matpr.2021.05.160>.
30. Dalaf, A. H., Jumaa, F. H., & Salih, H. K. (2021). Preparation, Characterization, Biological Evaluation and Assess Laser Efficacy for New Derivatives of Imidazolidin-4-one. *International Research Journal of Multidisciplinary Technovation*, **3(4)**, 41-51. <https://doi.org/10.34256/irjmt2145>.
31. Dalaf, A. H., Jumaa, F. H., & Salih, H. K. (2021). *MULTIDISCIPLINARY TECHNOVATION*. Red, **15(A2)**, C44H36N10O8.
32. Dalaf, A. H., Jumaa, F. H., Aftana, M. M., Salih, H. K., & Abd, I. Q. (2022). Synthesis, Characterization, Biological Evaluation, and Assessment Laser Efficacy for New Derivatives of Tetrazole. In *Key Engineering Materials* (Vol. 911, pp. 33-39). Trans Tech Publications Ltd. <https://doi.org/10.4028/p-6849u0>.
33. Naureen, B., Miana, G. A., Shahid, K., Asghar, M., Tanveer, S., & Sarwar, A. (2021). Iron (III) and zinc (II) monodentate Schiff base metal complexes: Synthesis, characterisation and biological activities. *Journal of Molecular Structure*, **1231**, 129946.

34. Alamro, F. S., Gomha, S. M., Shaban, M., Altowyan, A. S., Abolibda, T. Z., & Ahmed, H. A. (2021). Optical investigations and photoactive solar energy applications of new synthesized Schiff base liquid crystal derivatives. *Scientific reports*, *11*(1), 1-11.
35. Kaur, M., Kumar, S., Yusuf, M., Lee, J., Brown, R. J., Kim, K. H., & Malik, A. K. (2021). Post-synthetic modification of luminescent metal-organic frameworks using schiff base complexes for biological and chemical sensing. *Coordination Chemistry Reviews*, *449*, 214214.
36. Mahato, S., Meheta, N., Kotakonda, M., Joshi, M., Shit, M., Choudhury, A. R., & Biswas, B. (2021). Synthesis, structure, polyphenol oxidase mimicking and bactericidal activity of a zinc-schiff base complex. *Polyhedron*, *194*, 114933.